Generalized LED Index Modulation Optical OFDM for MIMO Visible Light Communications Systems

Ertuğrul Başar*, Erdal Panayirci*, Murat Uysal† and Harald Haas‡

*Istanbul Technical University, Faculty of Electrical and Electronics Engineering, 34469, Maslak, Istanbul, Turkey.
†Kadir Has University, Department of Electronics Engineering, 34083, Cibali, Istanbul, Turkey.
‡Ozyegin University, Department of Electrical and Electronics Engineering, 34794, Istanbul, Turkey.
§H. Haas is with the University of Edinburg, Institute for Digital Communications, Edinburg EH9 3JL, UK.
Email: basarer@itu.edu.tr, eepanay@khas.edu.tr, murat.uysal@ozyegin.edu.tr, h.haas@ed.ac.uk

***Abstract*—In this paper, we propose a generalized light emitting diode (LED) index modulation scheme for multiple input multiple output-orthogonal frequency division multiplexing (MIMO-OFDM) visible light communications (VLC) systems. The proposed scheme generalizes the LED index modulation concept by using the spatial multiplexing principle to transmit complex OFDM signals through VLC channels by separating these signals into their real-imaginary and positive-negative parts. The maximum a posteriori (MAP) estimator of the proposed scheme, which relies on quadratic programing (QP) problem, is presented for flat VLC channels. It is shown via computer simulations that the proposed scheme achieves considerably better error performance than the existing VLC-MIMO-OFDM systems due to its power efficiency and improved transceiver structure.**

I. Introduction

Visible light communications (VLC) is a promising new technology for next generation wireless communications systems due to its advantages over radio frequency (RF) based systems such as operation in unregulated wide spectrum and energy efficiency [1]. Light emitting diodes (LEDs) can be effectively used in indoor environments for both illumination and communications purposes. In order to provide adequate illumination, the use of multiple LEDs is very common in current indoor lighting setups, which can inherently lead to multiple-input multiple-output (MIMO) VLC systems [2]. Spatial modulation (SM), which is an effective MIMO solution, is adapted for VLC systems to achieve higher spectral efficiencies than single-input single-output (SISO) VLC systems [3]. Orthogonal frequency division multiplexing (OFDM) is also gaining attention for intensity modulation/direct detection (IM/DD) VLC systems due to its power efficiency and robustness to the intersymbol interference (ISI) [4].

In RF based OFDM systems, transmitted signals can be complex and bipolar; however, for IM/DD based VLC systems they must be real and positive since the intensity of the LEDs are modulated. This has been the major design challenge for VLC-OFDM systems and different approaches have been adopted to modify the classical OFDM for VLC systems. To make the resulting signal positive, either a direct current (DC) bias can be added on it as in the DC biased optical OFDM (DCO-OFDM) scheme or the signal can be clipped at zero level and only positive-valued signals are transmitted as in the asymmetrically clipped optical OFDM (ACO-OFDM) scheme, where both techniques have their advantages and disadvantages [4]. In order to solve the DC biasing problem of DCO-OFDM and to achieve higher spectral efficiency than ACO-OFDM, a non-DC-biased OFDM scheme (NDC-OFDM), which transmits the positive and negative signals from different LEDs, is proposed [5].

In this work, we propose a new optical OFDM scheme for MIMO-VLC systems, which does not require DC biasing/asymmetrical clipping and generalizes the LED index modulation concept using the spatial multiplexing principle. In the proposed generalized LED index modulation optical OFDM (GLIM-OFDM) scheme, complex signals are transformed to real-bipolar signals similar to [6]; however, these signals are then transmitted over MIMO channel in spatial multiplexing and LED index modulation fashion which is different from the single-input single-output (SISO) scheme of [6]. The maximum a posteriori (MAP) estimator of the proposed scheme is formulated and the superiority of the proposed scheme over its counterparts in bit error rate (BER) performance is shown via computer simulations.

The rest of the paper is organized as follows. In Section II, the system model of GLIM-OFDM is given. The conditional MAP estimator of the GLIM-OFDM scheme is presented in Section III. Simulation results are provided in Section IV. Finally, conclusions are given in Section V.

II. System Model of GLIM-OFDM

The block diagram of the GLIM-OFDM transmitter is given in Fig. 1. For the transmission of each OFDM block, the information bit vector $\mathbf{u}$, which contains $N\log_2(M)$ information bits, enters the GLIM-OFDM transmitter, where N is the number of OFDM subcarriers and M is the size of the considered signal constellation such as M-ary quadrature amplitude modulation (M-QAM). Opposite to DCO/ACO-OFDM and NDC-OFDM schemes, in the proposed scheme, the OFDM modulator directly processes the complex frequency-domain

This work is supported by the European Cooperation in Science and Technology (COST) - The Scientific and Technological Research Council of Turkey (TUBITAK) Research Grant No. 113E307.

978-1-4799-6664-6/16/$31.00 ©2016 IEEE

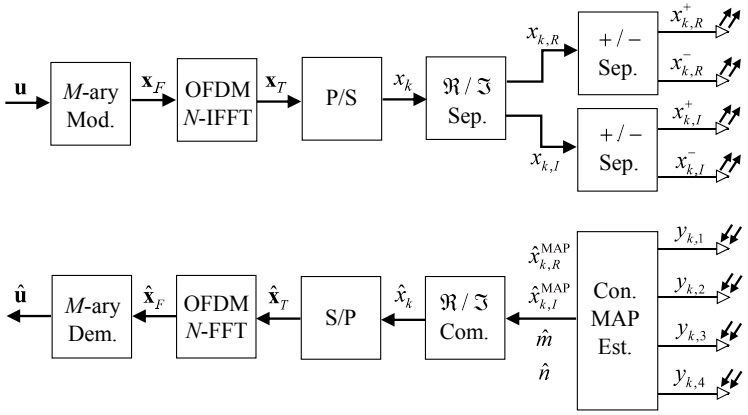

Fig. 1. Block Diagram of the GLIM-OFDM Scheme for a 4×4 MIMO-VLC System

OFDM frame $\mathbf{x}_F$. The resulting time-domain OFDM frame $\mathbf{x}_T = \begin{bmatrix} x_1 & \cdots & x_N \end{bmatrix}^T$ cannot be transmitted directly over a VLC channel because of its complex-valued and bipolar (positive and negative valued) elements. In order to overcome this problem, a new spatial multiplexing based MIMO transmission technique is developed. After parallel-to-serial (P/S) conversion, using a similar technique as in [6] for each OFDM signal for $k = 1, 2, \ldots, N$, first, the real and imaginary parts of the complex signal x_k are separated as $x_k = x_{k,R} + jx_{k,I}$. Afterwards, the resulting real, but bipolar signals $x_{k,R}$ and $x_{k,I}$ are applied to positive-negative $(+/-)$ separators to obtain the following positive-valued signals:

$$x^+_{k,R} = \begin{cases} x_{k,R} & \text{if } x_{k,R} > 0 \\ 0 & \text{if } x_{k,R} < 0 \end{cases} \quad x^-_{k,R} = \begin{cases} 0 & \text{if } x_{k,R} > 0 \\ -x_{k,R} & \text{if } x_{k,R} < 0 \end{cases}$$
$$x^+_{k,I} = \begin{cases} x_{k,I} & \text{if } x_{k,I} > 0 \\ 0 & \text{if } x_{k,I} < 0 \end{cases} \quad x^-_{k,I} = \begin{cases} 0 & \text{if } x_{k,I} > 0 \\ -x_{k,I} & \text{if } x_{k,I} < 0. \end{cases} \tag{1}$$

These positive-valued signals can be transmitted simultaneously from an $n_R \times n_T$ MIMO VLC system, where n_R and n_T denote the number of receiver (Rx) and transmitter (Tx) units, respectively, and $n_T = 4$ for the GLIM-OFDM scheme.

In the GLIM-OFDM scheme, LEDs transmit the absolute values of the $x_{k,R}$ and $x_{k,I}$ signals and the index of the transmitting LED determines the sign of the corresponding signals similar to the NDC-OFDM scheme; however, unlike NDC-OFDM, the use of spatial multiplexing concept for the real and imaginary parts of the complex OFDM signals, the spectral efficiency of the proposed scheme becomes $\log_2(M)$ [bits/s/Hz].

The positive and real-valued OFDM time samples $x^+_{k,R}, x^-_{k,R}, x^+_{k,I}$ and $x^-_{k,I}$ are transmitted over the $n_R \times 4$ optical MIMO channel (denoted by $\mathbf{H}$) for $k = 1, 2, \ldots, N$ as

$$\mathbf{y} = \mathbf{H}\mathbf{x} + \mathbf{n} \tag{2}$$

where $\mathbf{y} = \begin{bmatrix} y_{k,1} & \cdots & y_{k,n_R} \end{bmatrix}^T \in \mathbb{R}^{n_R \times 1}$ is the received signal vector which contains the electrical signals obtained from DD at the Rx units. Here, $\mathbf{n} \in \mathbb{R}^{n_R \times 1}$ is the real-valued additive white Gaussian noise (AWGN) vector, which models the shot noise and thermal noise. The elements of $\mathbf{n}$ follows $\mathcal{N}\left(0, \sigma_n^2\right)$ distribution, where $\mathcal{N}(\mu, \sigma^2)$ denotes the normal distribution with mean μ and variance σ^2, and are added to the received signals at the electrical domain. The transmitted signal vector $\mathbf{x} \in \mathbb{R}^{4 \times 1}$ is formed for GLIM-OFDM as

$$\mathbf{x} = \begin{bmatrix} x^+_{k,R} & x^-_{k,R} & x^+_{k,I} & x^-_{k,I} \end{bmatrix}^T \tag{3}$$

where the elements of $\mathbf{x}$ indicate the signals emitted by the LEDs. According to (1), for a given OFDM signal, only two out of four elements of $\mathbf{x}$ are non-zero, i.e., two LEDs are active (emitting light) while the other two LEDs remain inactive (turned off). In this study, we consider $n_R = 4$ for ease of presentation while a generalization is straightforward. We assume that LEDs are operating within the dynamic range. Note that the operation in (1) is not subject to non-linear distorsions.

The 4×4 optical MIMO channel is represented by

$$\mathbf{H} = \begin{bmatrix} h_{1,1} & h_{1,2} & h_{1,3} & h_{1,4} \\ h_{2,1} & h_{2,2} & h_{2,3} & h_{2,4} \\ h_{3,1} & h_{3,2} & h_{3,3} & h_{3,4} \\ h_{4,1} & h_{4,2} & h_{4,3} & h_{4,4} \end{bmatrix} \tag{4}$$

where $h_{r,t}$ denotes the channel gain of the optical wireless link between the Tx unit (LED) t and the Rx unit (PD) r, where $(t, r) \in \{1, 2, 3, 4\}$. In this study, we consider line-of-sight (LOS) optical transmission links between Tx's and Rx's due to their simplicity. Interested readers are referred to [3] and [7] for more advanced channel models. The elements of $\mathbf{H}$ can be calculated for our channel model as follows:

$$h_{r,t} = \begin{cases} \frac{(m+1)A_r}{2\pi d_{r,t}^2} \cos^m(\phi_t)\, T_s(\psi_r) \cos(\psi_r), & 0 \le \psi_r \le \Psi_c \\ 0, & \psi_r > \Psi_c \end{cases} \tag{5}$$

where $m = -\ln 2 / \ln(\cos \Phi_{1/2})$ is the order of the Lambertian emission, $\Phi_{1/2}$ is the Tx semiangle, A_r is the physical detector area of the receiver, $d_{r,t}$ is the distance between Tx t and Rx r, ϕ_t and ψ_r denote the angles of emergence and incidence with respect to the Tx and Rx axes, respectively. Ψ_c is the field-of-view (FOV) semiangle of the PD. $T_s(\psi_r)$ is the optical filter

gain which is assumed to be unity in this work. Additionally, we assume the following parameters in this study: $\Phi_{1/2} = \Psi_c = 15^\circ, A_r = 1\,\text{cm}^2$.

As seen from (5), the corresponding channel gain coefficients between Tx's and Rx's are closely related to the angles of ϕ_t and ψ_r which are determined according to the specific positions of the Tx's and Rx's. Furthermore, (5) also states that $h_{r,t} = 0$ if Rx r is not in the FOV of Tx t.

In this study, we consider the average electrical signal-to-noise ratio (SNR) at each Rx unit, which is defined as [3]

$$\text{SNR} = \frac{P_{\text{Rx}}^{\text{E}}}{\sigma_n^2} = \frac{1}{\sigma_n^2}\left(\frac{1}{n_R}\sum\nolimits_{r=1}^{n_R} P_{\text{Rx}}^{\text{O}}\right)^2 \tag{6}$$

where P_{Rx}^{E} is the average received electrical power,

$$P_{\text{Rx}}^{\text{O}} = \sum\nolimits_{t=1}^{n_T} h_{r,t} I \tag{7}$$

is the average received optical power at receive unit r and I is the mean optical intensity being emitted. Please note that there is not a consensus for the definition of SNR in VLC community and the model in (5) is considered to work on reasonable SNR regions as in [3] and [5]. Let us assume that $\text{E}\left\{\mathbf{x}_F^H \mathbf{x}_F\right\} = N$, i.e., M-QAM constellation is normalized to have unit-energy symbols. It can be shown that the elements of $\mathbf{x}_T$ follows $\mathcal{CN}(0,1)$ distribution for large N values if inverse fast Fourier transform (IFFT) operation satisfies the normalization of $\text{E}\left\{\mathbf{x}_T^H \mathbf{x}_T\right\} = N$, where $\mathcal{CN}(0,\sigma^2)$ denotes the circularly symmetrical Gaussian distribution with variance σ^2. Considering that $x_{k,R}$ and $x_{k,I} \sim \mathcal{N}(0,1/2)$, due to the symmetry, all four elements of $\mathbf{x}$ have the following clipped Gaussian probability density function (p.d.f.)

$$p_{x_{k,R(I)}^{\pm}}(v) = (1/\sqrt{\pi})\exp\left(-v^2\right)u(v) + \frac{1}{2}\delta(v) \tag{8}$$

where $u(v)$ and $\delta(v)$ denote unit step and Dirac delta functions, respectively. Then, the average optical power emitted from the LED of GLIM-OFDM scheme is obtained as

$$I = \int_0^\infty v p_{x_{k,R(I)}^{\pm}}(v)dv = 1/(2\sqrt{\pi}). \tag{9}$$

III. Conditional MAP Estimator of GLIM-OFDM

The transmission model given in (2) resembles that of the classical single-carrier MIMO-SM systems; however, it differs from this model in two main points: Firstly, the received signals are real in (2) and secondly the transmitted data vector $\mathbf{x}$ has a clipped Gaussian distribution. Furthermore, it is not possible to forward the received signal vector $\mathbf{y}$ to the OFDM demodulator directly, due to the fact that complex valued signals must be constructed first to obtain the estimate of the frequency domain OFDM block $\mathbf{x}_F$. A straightforward solution to the detection problem formulated in (2) is the use of the zero-forcing (ZF) estimator which yields an estimate of $\mathbf{x}$ simply as

$$\hat{\mathbf{x}}^{\text{ZF}} = \mathbf{H}^{-1}\mathbf{y}. \tag{10}$$

Afterwards, the receiver can determine the indices of the active LEDs and corresponding signals by selecting the higher magnitude signals from $\hat{\mathbf{x}}^{\text{ZF}}$ [5]. Despite its simplicity, the ZF estimator can significantly enhance the noise power through multiplication of $\mathbf{n}$ with $\mathbf{H}^{-1}$; furthermore, it does not consider the probability distribution of $\mathbf{x}$ as a *a priori* information and consequently, it may produce negative-valued estimates. To overcome the aforementioned drawbacks of the ZF estimator, in this section we propose a MAP estimator for the GLIM-OFDM scheme by taking into account the prior information we have for the signal vector $\mathbf{x}$.

Defining the column vectors of $\mathbf{H}$ as $\mathbf{H} = \begin{bmatrix}\mathbf{h}_1 & \mathbf{h}_2 & \mathbf{h}_3 & \mathbf{h}_4\end{bmatrix}$, the observed signal given in (2) can be rewritten as

$$\mathbf{y} = \mathbf{h}_m \bar{x}_{k,R} + \mathbf{h}_n \bar{x}_{k,I} + \mathbf{n} \tag{11}$$

where $\bar{x}_{k,R} = |x_{k,R}|$, $\bar{x}_{k,I} = |x_{k,I}|$, $m \in \{1,2\}$ and $n \in \{3,4\}$. It can be easily shown that $\bar{x}_{k,R}$ and $\bar{x}_{k,I}$ have a folded Gaussian (half-normal) distribution with

$$p_{\bar{x}_{k,R(I)}}(v) = (2/\sqrt{\pi})\exp(-v^2)u(v). \tag{12}$$

Consequently, for a given pair (m,n), the conditional MAP estimates of $\bar{x}_{k,R}$ and $\bar{x}_{k,I}$ can be obtained as

$$\left(\tilde{x}_{k,R}^{(m,n)}, \tilde{x}_{k,I}^{(m,n)}\right) = \arg\max_{\bar{x}_{k,R},\bar{x}_{k,I}} p\left(\bar{x}_{k,R}, \bar{x}_{k,I} \,|\, \mathbf{y}\right) \tag{13}$$

where $p\left(\bar{x}_{k,R}, \bar{x}_{k,I} \,|\, \mathbf{y}\right)$ is the probability density function (p.d.f.) of $\bar{x}_{k,R}$ and $\bar{x}_{k,I}$, conditioned on $\mathbf{y}$. Using Bayes' rule, and considering that $\bar{x}_{k,R}$ and $\bar{x}_{k,I}$ are independent, (13) can be rewritten as

$$\left(\tilde{x}_{k,R}^{(m,n)}, \tilde{x}_{k,I}^{(m,n)}\right) = \arg\max_{\bar{x}_{k,R},\bar{x}_{k,I}} p\left(\mathbf{y}|\, \bar{x}_{k,R}, \bar{x}_{k,I}\right) p(\bar{x}_{k,R}) p(\bar{x}_{k,I}). \tag{14}$$

Since the conditional distribution of $\mathbf{y}$, given $\bar{x}_{k,R}$, $\bar{x}_{k,I}$ and (m,n) is $\mathcal{N}\left(\mathbf{h}_m \bar{x}_{k,R} + \mathbf{h}_n \bar{x}_{k,I}, \sigma_n^2\right)$, by dropping constant terms from (14), we obtain

$$\begin{aligned}\left(\tilde{x}_{k,R}^{(m,n)}, \tilde{x}_{k,I}^{(m,n)}\right) = \arg\max_{\bar{x}_{k,R},\bar{x}_{k,I}} &\exp\left(-\left[\bar{x}_{k,R}^2 + \bar{x}_{k,I}^2\right]\right) \\ &\times \exp\left(-\left\|\mathbf{y} - \mathbf{h}_m \bar{x}_{k,R} - \mathbf{h}_n \bar{x}_{k,I}\right\|^2 / \left(2\sigma_n^2\right)\right).\end{aligned} \tag{15}$$

Taking the logarithm of (15) with simple manipulations, it follows that

$$\left(\tilde{x}_{k,R}^{(m,n)}, \tilde{x}_{k,I}^{(m,n)}\right) = \arg\min_{\bar{x}_{k,R},\bar{x}_{k,I}} M^{\text{MAP}}(m,n,\bar{x}_{k,R},\bar{x}_{k,I}). \tag{16}$$

where $M^{\text{MAP}}\left(m,n,\bar{x}_{k,R},\bar{x}_{k,I}\right)$ is the MAP estimation metric defined as

$$\begin{aligned}M^{\text{MAP}}\left(m,n,\bar{x}_{k,R},\bar{x}_{k,I}\right) = &\left\|\mathbf{y} - \mathbf{h}_m \bar{x}_{k,R} - \mathbf{h}_n \bar{x}_{k,I}\right\|^2 \\ &+ 2\sigma_n^2\left(\bar{x}_{k,R}^2 + \bar{x}_{k,I}^2\right).\end{aligned} \tag{17}$$

Using $\|\mathbf{a}\|^2 = \mathbf{a}^T\mathbf{a}$ and after some algebra, (17) can be simplified as

$$\begin{aligned}&M^{\text{MAP}}\left(m,n,\bar{x}_{k,R},\bar{x}_{k,I}\right) = \\ &\quad A\bar{x}_{k,R}^2 + B\bar{x}_{k,I}^2 + C\bar{x}_{k,R} + D\bar{x}_{k,I} + E\bar{x}_{k,R}\bar{x}_{k,I}\end{aligned} \tag{18}$$

where

$$\begin{aligned}A &= \mathbf{h}_m^T\mathbf{h}_m + 2\sigma_n^2 \qquad B = \mathbf{h}_n^T\mathbf{h}_n + 2\sigma_n^2 \\ C &= -2\mathbf{y}^T\mathbf{h}_m \qquad D = -2\mathbf{y}^T\mathbf{h}_n \\ &E = 2\mathbf{h}_m^T\mathbf{h}_n.\end{aligned} \tag{19}$$

For $\mathbf{q} = \left[\bar{x}_{k,R} \;\; \bar{x}_{k,I}\right]^T$, it is observed that the minimization of (18) is equivalent to a well-known constraint quadratic programming (QP) problem defined as [8]

$$\min_{\mathbf{q}} \left\{ \frac{1}{2}\mathbf{q}^T\mathbf{Q}\mathbf{q} + \mathbf{c}^T\mathbf{q} \right\} \qquad \text{subject to} \;\; \mathbf{A}\mathbf{q} \preceq \mathbf{b} \tag{20}$$

for $\mathbf{Q}$ being a real and symmetric matrix. (20) can be efficiently solved by defining

$$\mathbf{Q} = \begin{bmatrix} 2A & E \\ E & 2B \end{bmatrix}, \quad \mathbf{c} = \begin{bmatrix} C \\ D \end{bmatrix}, \tag{21}$$

$$\mathbf{A} = \begin{bmatrix} -1 & 0 \\ 0 & -1 \end{bmatrix}, \quad \mathbf{b} = \begin{bmatrix} 0 \\ 0 \end{bmatrix}. \tag{22}$$

Note that the optimal estimate of $\mathbf{q}$ also guarantees that $\tilde{x}_{k,R}^{(m,n)} \geq 0$ and $\tilde{x}_{k,I}^{(m,n)} \geq 0$ for all $\mathbf{Q}$ and $\mathbf{c}$, i.e. regardless of the SNR and the channel conditions. In other words, the proposed conditional MAP-QP estimator always gives positive-valued estimates of $\bar{x}_{k,R}$ and $\bar{x}_{k,I}$ regardless of SNR and channel conditions.

In order to determine the indices of the active LEDs (i.e. estimations of m and n) as well as the corresponding estimates of $\bar{x}_{k,R}$ and $\bar{x}_{k,I}$, the conditional MAP estimator obtains $\tilde{x}_{k,R}^{(m,n)}$ and $\tilde{x}_{k,I}^{(m,n)}$ for all possible (m,n) pairs, and then obtains the unconditional (actual) estimates of $\bar{x}_{k,R}$ and $\bar{x}_{k,I}$ as follows:

$$(\hat{m},\hat{n}) = \arg\min_{m,n} M^{\text{MAP}}\left(m,n,\tilde{x}_{k,R}^{(m,n)},\tilde{x}_{k,I}^{(m,n)}\right),$$
$$\hat{x}_{k,R}^{\text{MAP}} = \tilde{x}_{k,R}^{(\hat{m},\hat{n})}, \quad \hat{x}_{k,I}^{\text{MAP}} = \tilde{x}_{k,I}^{(\hat{m},\hat{n})}. \tag{23}$$

In other words, after the calculation of the MAP estimates of $\bar{x}_{k,R}$ and $\bar{x}_{k,I}$ for all (m,n), $(m,n) \in \{(1,3),(1,4),(2,3),(2,4)\}$ which considers all possible active LED scenarios, the conditional MAP estimator of the GLIM-OFDM scheme decides on the most likely active LED pair $(\hat{m},\hat{n})$ and corresponding estimates of $\bar{x}_{k,R}$ and $\bar{x}_{k,I}$ $(\hat{x}_{k,R}^{\text{MAP}},\hat{x}_{k,I}^{\text{MAP}})$ by calculating the MAP estimation metric given in (17) for all four scenarios. Then, the $\Re/\Im$ combiner calculates the estimate of the complex OFDM signal x_k as

$$\hat{x}_{k,R} = \begin{cases} \hat{x}_{k,R}^{\text{MAP}}, & \text{if } m=1 \\ -\hat{x}_{k,R}^{\text{MAP}}, & \text{if } m=2 \end{cases} \qquad \hat{x}_{k,I} = \begin{cases} \hat{x}_{k,I}^{\text{MAP}}, & \text{if } n=3 \\ -\hat{x}_{k,I}^{\text{MAP}}, & \text{if } n=4 \end{cases} \tag{24}$$

After this point, classical OFDM procedures are applied to obtain the estimate $\hat{\mathbf{u}}$ of the information bit vector $\mathbf{u}$.

IV. Simulation Results

We consider a 4×4 MIMO-VLC system operating in a typical room with $3\,\text{m} \times 3\,\text{m} \times 2.5\,\text{m}$ dimensions where the Tx's and Rx's are located at a height of $2.25\,\text{m}$ and $0.75\,\text{m}$, respectively. Four Tx's and Rx's are aligned in square 2×2 arrays with $d_{Tx} \times d_{Tx}$ and $d_{Rx} \times d_{Rx}$ dimensions, respectively, and centered right in the middle of the room. The Tx's and Rx's are oriented straight down to the floor and straight up to the ceiling, respectively. We assume that d_{Rx} is fixed and set to $d_{Rx} = 0.15\,\text{m}$, while we investigate the performance of the proposed scheme with varying $d_{Tx} \in \{0.3\,\text{m}, 0.45\,\text{m}, 0.6\,\text{m}\}$,

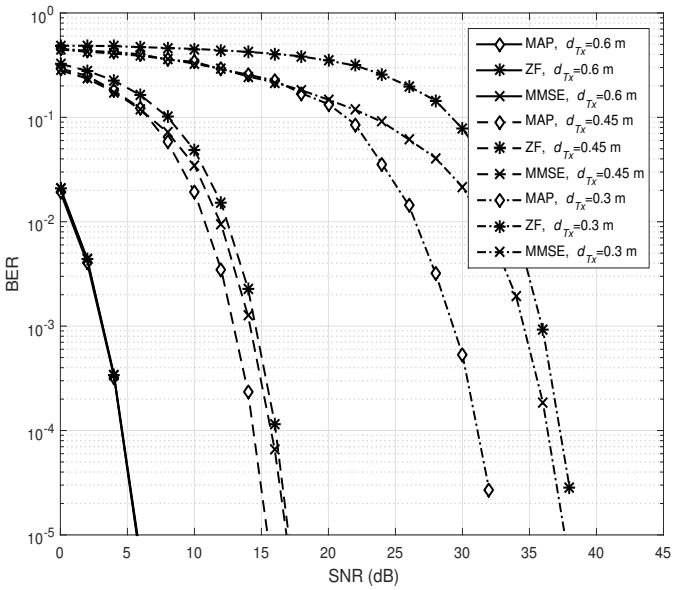

Fig. 2. BER performance of MAP and ZF/MMSE estimators for 2 bits/s/Hz

which correspond to $\mathbf{H}$ matrices with highly, moderately and slightly similar elements, respectively.

We compare the BER performance of the proposed scheme with the 2×2 NDC-OFDM [5], 4×4 OSM-OFDM-ACO, 4×4 OSM-OFDM-DCO schemes, which combine optical spatial modulation (OSM) [3] and optical OFDM [4], and 4×4 vertical Bell Labs layered space-time (V-BLAST) type OFDM-ACO scheme [2] with respect to average received electrical SNR. Spectral efficiencies of these schemes are $(1/2)\log_2(M)$, $(1/4)\log_2(4M)$, $(1/2)\log_2(4M)$ and $\log_2(M)$ [bits/s/Hz], respectively. For these four schemes, the ZF estimator is used as in [5], while the development of MAP estimators for these schemes is beyond the scope of this study. The following I values are considered in our computer simulations: $1/\sqrt{2\pi}$, $1/(4\sqrt{\pi})$, $\frac{\sigma_x}{2\pi}\exp(-B_{DC}^2/(2\sigma_x^2)) + B_{DC}(1-Q(B_{DC}/\sigma_x))$, $1/(2\sqrt{\pi})$, where $\sigma_x^2 = 1/n_T$ is the variance of the time-domain OFDM signal at each branch of the OSM-OFDM-DCO transmitter. B_{DC} is the DC bias value which is defined as in [4]. To make fair comparisons, we also consider the two-parallel NDC-OFDM (P-NDC-OFDM) scheme for $n_T = n_R = 4$ with $\log_2(M)$ [bits/s/Hz] spectral efficiency.

In Fig. 2, we compare the the BER performance of the MAP, ZF and minimum mean square error (MMSE) estimators of the proposed scheme with varying d_{Tx} values. As seen from Fig. 2, for $d_{Tx} = 0.6$, the ZF/MMSE and MAP estimators provide the same performance since $\mathbf{H}$ is as a diagonal matrix for this case (aligned system), and there is no need to use complex estimators at the Rx to obtain $\hat{x}_k$. On the other hand, with decreasing d_{Tx} (for higher similarities in $\mathbf{H}$), the superiority of the MAP estimator becomes more evident.

In Fig. 3, computer simulation results are presented for the proposed scheme, OSM-OFDM-DCO, OSM-OFDM-ACO,

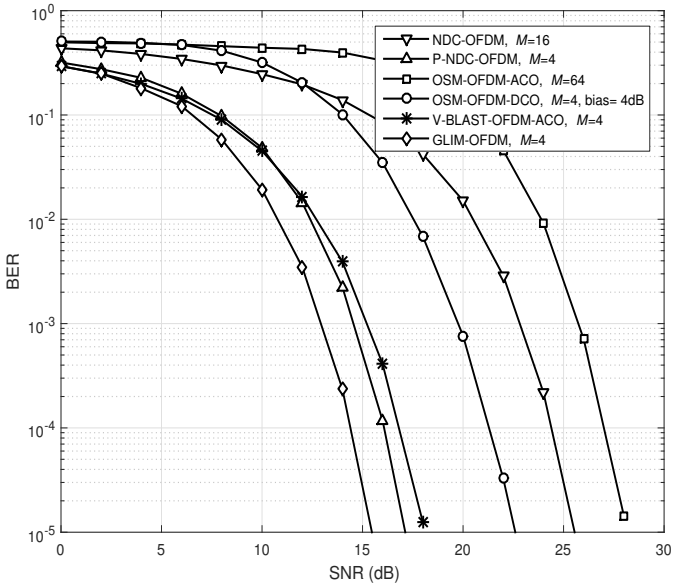

Fig. 3. BER performance comparison of optical MIMO-OFDM schemes for 2 bits/s/Hz

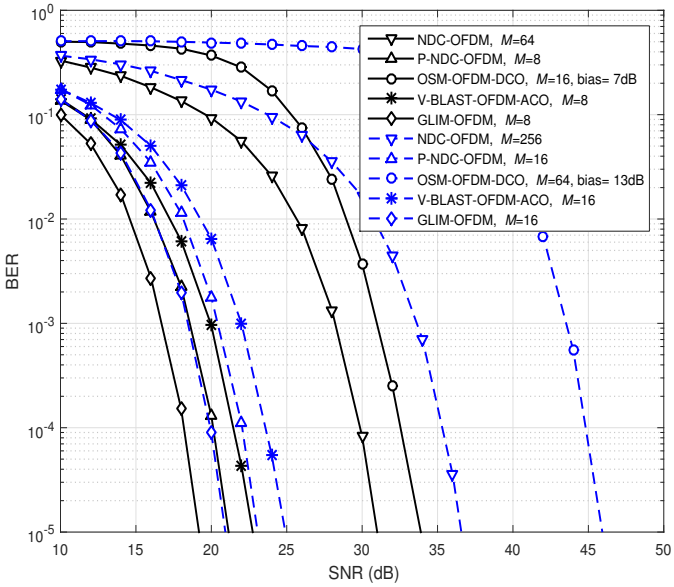

Fig. 4. BER performance comparison of optical MIMO-OFDM schemes for $3-4$ bits/s/Hz

(P)-NDC-OFDM and V-BLAST-OFDM-ACO schemes at 2 bits/s/Hz for $d_{Tx} = 0.45$. As seen from Fig. 3, the GLIM-OFDM scheme exhibits better BER performance than all of the reference schemes due to its power efficiency which is the result of the employment of lower order modulation to reach the target spectral efficiency, and its powerful MAP estimator.

In Fig. 4, we show the BER performance curves of the proposed scheme, OSM-OFDM-DCO, (P)-NDC-OFDM and V-BLAST-OFDM-ACO schemes at $3-4$ bits/s/Hz spectral efficiencies for $d_{Tx} = 0.45$. As seen from Fig. 4, the BER performance advantage of GLIM-OFDM over lower rate reference schemes increases for $3-4$ bits/s/Hz since these power inefficient schemes use higher order modulations to reach the same spectral efficiency.

V. Conclusions and Future Work

MIMO technology is inherently available for VLC systems due to off-the-shelf multi-chip LEDs which do not increase the hardware complexity of the system. A new optical MIMO-OFDM scheme has been proposed in this paper. By using spatial multiplexing principle, the proposed GLIM-OFDM scheme can transmit complex OFDM signals through optical channel by means of the separated signal components consisting of their real-imaginary and positive-negative parts. As a future study, we plan to modify this system to operate on frequency selective VLC channels to cope with the ISI.

References

[1] S. Wu, H. Wang, and C.-H. Youn, "Visible light communications for 5G wireless networking systems: from fixed to mobile communications," *IEEE Network*, vol. 28, no. 6, pp. 41–45, Nov. 2014.

[2] T. Fath and H. Haas, "Performance comparison of MIMO techniques for optical wireless communications in indoor environments," *IEEE Trans. Commun.*, vol. 61, no. 2, pp. 733–742, Feb. 2013.

[3] R. Mesleh, H. Elgala, and H. Haas, "Optical spatial modulation," *IEEE/OSA J. Opt. Commun. Netw.*, vol. 3, no. 3, pp. 234–244, Mar. 2011.

[4] S. Dissanayake and J. Armstrong, "Comparison of ACO-OFDM, DCO-OFDM and ADO-OFDM in IM/DD systems," *J. Lightw. Technol.*, vol. 31, no. 7, pp. 1063–1072, Apr. 2013.

[5] Y. Li, D. Tsonev, and H. Haas, "Non-DC-biased OFDM with optical spatial modulation," in *IEEE Int. Symp. Personal Indoor and Mobile Radio Commun.*, Sep. 2013, pp. 486–490.

[6] A. Nuwanpriya, A. Grant, S.-W. Ho, and L. Luo, "Position modulating OFDM for optical wireless communications," in *IEEE Globecom Workshops*, Dec. 2012, pp. 1219–1223.

[7] J. Kahn and J. Barry, "Wireless infrared communications," *Proc. IEEE*, vol. 85, no. 2, pp. 265–298, Feb. 1997.

[8] S. Boyd and L. Vandenberghe, *Convex Optimization*. Cambridge University Press, 2004.